Published in final edited form as:
Oncogene. 2010 July 15; 29(28): 4113–4120. doi:10.1038/onc.2010.150.

Genetic reporter system for oncogenic *Igh–Myc* translocations in mice

M Takizawa[1,2,6], **JS Kim**[1,6,7], **L Tessarollo**[3], **N McNeil**[4], **TJ Waldschmidt**[5], **R Casellas**[2], **T Ried**[4], and **S Janz**[5]

[1]Laboratory of Genetics, Center for Cancer Research (CCR), National Cancer Institute (NCI), Bethesda, MD, USA

[2]Genomics & Immunity, National Institute of Arthritis and Musculoskeletal Disease, Bethesda, MD, USA

[3]Mouse Cancer Genetics Program, CCR, NCI, Bethesda, MD, USA

[4]Genetics Branch, CCR, NCI, National Institutes of Health, Bethesda, MD, USA

[5]Department of Pathology, The University of Iowa Roy J and Lucille A Carver College of Medicine, Iowa City, IA, USA

Abstract

The *Myc*-deregulating chromosomal T(12;15)(*Igh–Myc*) translocation, the hallmark mutation of inflammation- and interleukin 6-dependent mouse plasmacytoma (PCT), is the premier model of cancer-associated chromosomal translocations because it is the only translocation in mice that occurs spontaneously (B lymphocyte lineage) and with predictably high incidence (~85% of PCT), and has a direct counterpart in humans: Burkitt lymphoma t(8;14)(q24;q32) translocation. Here, we report on the development of a genetic system for the detection of T(12;15)(*Igh–Myc*) translocations in plasma cells of a mouse strain in which an enhanced green fluorescent protein (GFP)-encoding reporter gene has been targeted to *Myc*. Four of the PCTs that developed in the newly generated translocation reporter mice, designated iGFP$^{5'Myc}$, expressed GFP consequent to naturally occurring T(12;15) translocation. GFP expression did not interfere with tumor development or the deregulation of *Myc* on derivative 12 of translocation, der (12), because the reporter gene was allocated to the reciprocal product of translocation, der (15). Although the described reporter gene approach requires refinement before T(12;15) translocations can be quantitatively detected *in vivo*, including in B lymphocyte lineage cells that have not yet completed malignant transformation, our findings provide proof of principle that reporter gene tagging of oncogenes in gene-targeted mice can be used to elucidate unresolved questions on the occurrence, distribution and trafficking of cells that have acquired cancer-causing chromosomal translocations of great relevance for humans.

Correspondence: Professor S Janz, Department of Pathology, The University of Iowa Roy J and Lucille A Carver College of Medicine, 500 Newton Road, 1046C ML, Iowa City, IA 52246, USA., siegfried-janz@uiowa.edu.
[6]These authors contributed equally to this work.
[7]Current address: Korea Research Institute of Bioscience and Biotechnology (KRIBB), 52 Oun, Yusong, Taejon 305–333, Republic of Korea.

Conflict of interest

The authors declare no conflict of interest.

Supplementary Information accompanies the paper on the Oncogene website (http://www.nature.com/onc)

Keywords

mouse plasmacytoma T(12;15) translocation; human Burkitt lymphoma t(8;14)(q24;q32) translocation; green fluorescence protein

Reciprocal chromosomal translocations that illegitimately recombine cellular oncogenes with immunoglobulin genes have long been recognized as hallmarks of both B-cell and plasma-cell neoplasms in humans (Willis and Dyer, 2000; Kuppers and Dalla-Favera, 2001). The t(8;14)(q24;q32) translocation, most commonly observed in the post-germinal center B-cell tumor, Burkitt lymphoma, is of special interest because it results in the deregulated expression of a gene that is among the most important cancer genes—*MYC* (Eisenman, 2001; Levens, 2003); it is the first cancer-associated translocation to have been characterized at the molecular level—balanced (reciprocal) genetic exchange of *MYC* with the Ig heavy-chain locus, *IGH* (Dalla-Favera *et al.*, 1982); it is widely believed to be a very early, if not initiating, transforming event in neoplastic B-cell development; and, unlike the great majority of oncogene-activating translocations found in human lymphoma and leukemia, it has a direct counterpart in mice—T(12;15)(*Igh–Myc*)—that is itself the hallmark of peritoneal BALB/c plasmacytoma (PCT). Like human t(8;14)(q24;q32) in Burkitt lymphoma, mouse T(12;15) in PCT is thought to be a tumor-initiating mutation (Janz *et al.*, 1993). Despite exciting recent progress in our understanding of the molecular mechanism that underlies *Igh–Myc* translocation (Ramiro *et al.*, 2004; Robbiani *et al.*, 2008; Wang *et al.*, 2009; Gostissa *et al.*, 2009b), fundamental questions on the biology of this translocation remain unresolved, primarily because of the difficulty in detecting individual translocation-bearing cells *in vivo*.

We have taken an important first step to overcome this difficulty by developing a genetic method for the detection of individual T(12;15)-carrying cells in mice. Using established gene-targeting methods in embryonic stem cells, we generated iGFP$^{5'Myc}$ gene-insertion mice that harbor in the near upstream flank of the *Myc* locus a cDNA gene that encodes the enhanced GFP protein under control of the mouse immunoglobulin heavy-chain (*Igh*) variable gene promoter, V_H (Figure 1, top). The GFP reporter has been inserted ~1.5 kb 5′ of *Myc* exon 1, to make it possible to specifically detect derivative 15, der(15), of the T(12;15) translocation. Unlike der(12), which contains the deregulated *Myc* gene that drives tumor development (Eisenman, 2001; Levens, 2003) and is subject to secondary changes in the course of plasmacytomagenesis, including those caused by class switch recombination on the rearranged *Igh–Myc* domain (Kovalchuk *et al.*, 1997), der(15) is thought to be inconsequential for malignant cell transformation and not affected by secondary structural modification. Moreover, cytogenetic analysis of hundreds of mouse PCTs has shown that der(15) is rarely, if ever, lost in T(12;15)$^+$ tumors. These features render der(15) a particularly attractive host for a translocation reporter gene, such as the V_H-GFP that we use here. Because the GFP gene insertion site in iGFP$^{5'Myc}$ mice is just upstream of the known 5′ boundary of the translocation breakpoint cluster in *Myc*, the reporter gene will invariably be allocated to der(15), irrespective of the actual break site in *Myc*, which occurs in most cases in intron 1 or exon 1 of the gene and, less frequently, in its near 5′ flank.

According to the scheme presented in Figure 1, GFP remains silent in B cells of strain iGFP$^{5'Myc}$ mice that have not undergone T(12;15) exchange because the V_H promoter of the GFP gene on chromosome 15 cannot be activated in *trans* by *Igh* enhancers on chromosome 12 (Figure 1, top). However, in B cells that do undergo T(12;15) exchange (Figure 1, bottom), GFP is expressed upon the juxtaposition of V_H–GFP to an *Igh* enhancer in *cis*. Assembly of the targeting vector, generation of iGFP$^{5'Myc}$ ‘knock-in’ mice, and the

development of genomic PCR methods for genotyping transgenic off-spring are described online in Supplementary Methods and illustrated in Supplementary Figure 1.

Reporter genes targeted to oncogenes may either promote or inhibit tumorigenesis—by changing the structure, accessibility or biological function of the modified genetic loci. To evaluate whether either is true in the case of strain iGFP$^{5'Myc}$, we performed a PCT induction study in these mice. To accelerate tumor development, we combined the iGFP$^{5'Myc}$ reporter gene with a human *BCL2* transgene that was shown in previous work to lead to T(12;15)-harboring plasma cell tumors with short onset and full penetrance (Silva *et al.*, 2003). Figure 2 shows that upon induction of chronic peritoneal inflammation using pristane (Anderson and Potter, 1969), PCTs arose as rapidly (onset 50–120 days) and with the same incidence (100%) in double-transgenic iGFP$^{5'Myc}$/BCL2 mice as in single-transgenic BCL2 mice. Characteristic features of mouse PCTs that are detectable by histomorphological criteria, by the expression of certain cell-surface markers including CD138 and by monoclonal Ig production, were also indistinguishable in iGFP$^{5'Myc}$/BCL2 and BCL2 mice (results not shown).

To evaluate whether the proclivity of PCT to undergo T(12;15) translocation was comparable in iGFP$^{5'Myc}$-transgenic mice and mice lacking the reporter transgene, we employed genomic PCR to analyze 13 tumors from iGFP$^{5'Myc}$/BCL2 mice for the presence of chimeric *Igh–Myc* junction fragments (Kovalchuk *et al.*, 2000b). The remaining six tumors included in Figure 2 were not available for molecular studies. Using the *Myc* and *Igh* primers depicted in Figure 1, we readily detected T(12;15)-typical junctions in 11 of 13 PCTs: der(12)-typical junctions were found in 10 tumors, and der(15)-typical junctions were seen in nine (Table 1, columns 3–4). The translocation status of two tumors remained undetermined, presumably because they contained an unusual T(12;15) exchange that was not detectable with the PCR methods used here, harbored a variant *Myc* translocation that relied on an immunoglobulin light-chain instead of the *Igh* locus, or did not harbor an *Myc* translocation at all. The detection of T(12;15) in 85% of iGFP$^{5'Myc}$-carrying PCT was consistent with the incidence of this translocation in PCTs from normal mice of strain C (Janz, 2006).

The results presented above suggested that the GFP reporter gene in strain iGFP$^{5'Myc}$ is a passive genomic passenger that neither affects PCT development nor diminishes the likelihood that the T(12;15) translocation will be generated. However, because the present sample of translocation-bearing tumors is small (n = 11), a follow-up study producing a larger data set is necessary before it can be unambiguously decided whether the GFP reporter does or does not cause bias with regard to translocation occurrence and tumor development. Including a side-by-side comparison of hemizygous transgenic iGFP$^{5'Myc}$ mice (containing one targeted and one normal *Myc* locus) and their homozygous transgenic counterparts (lacking the normal *Myc* locus) in that study may be particularly informative.

To identify PCTs in which T(12;15) is associated with GFP expression, we performed FACS analysis of the 11 tumors that showed PCR-based evidence of translocation. We stained PCT-containing ascites specimens with antibody to CD138 (syndecan-1, marker of plasma cells) and B220 (CD45R, marker of B cells) to distinguish the malignant plasma cells from populations of normal cells including peritoneal B cells. We found that 4 of 11 (36%) tumors expressed high levels of GFP (Table 1, column 2). This is illustrated in Figure 3a, in which PCT2 serves as a GFP$^+$ example, and PCT8 as a GFP$^-$ example. In the case of PCT2, 24% of ascites cells were neoplastic plasma cells, as indicated by the co-expression of GFP and CD138 (GFP$^+$CD138$^+$) and a lack of B220 expression (B220$^-$). The fraction of GFP$^+$ tumor cells in the three other cases characterized by high levels of GFP (PCT1, 3, 4) ranged from 6 to 31% (Supplementary Figure 2). To confirm GFP expression in these cells

by an independent method that additionally provides insight into the location and distribution of translocation-bearing cells *in vivo*, we performed immunofluorescence microscopy with antibodies to CD138 and B220, on serial tissue sections of peritoneal granulomas, the sites of PCT development. In all four cases (PCT1–4), GFP^+CD138^+ tumor cells that infiltrated the granulomatous tissue (Figure 3b, top and bottom rows) were readily distinguished from GFP^-B220^+ B lymphocytes (Figure 3b, center row). Normal $CD138^+$ plasmablasts and plasma cells residing in spleen, gut villi and bone marrow were GFP-negative (not shown).

To further show that GFP expression in PCT1–4 was caused by the T(12;15) translocation, we performed fluorescence *in situ* hybridyzation (FISH) of *Myc* and *Igh* as described in Supplementary Methods. FISH detects distinct *Myc* and *Igh* signals in normal cells, but a co-localized or merged *Igh–Myc* signal in $T(12;15)^+$ cells. In the case of PCT1, 11 of 15 (73%) tumor cells analyzed at the metaphase stage of the cell cycle showed merged FISH signals on der(12) (Figure 3c). In the case of PCT2, this was true for 10 of 10 (100%) tumor cells. As PCT3 and PCT4 contained less than the 10 metaphase cells commonly required for reliable cytogenetic diagnosis, we analyzed these tumors by interphase FISH. In the case of PCT3, co-localization of *Myc* and *Igh* signals was seen in 34 of 154 (22.1%) cells from an ascites specimen that contained 35% tumor cells and 65% normal (mostly inflammatory) cells (Supplementary Figure 3). The observed co-localization frequency was significantly elevated compared with that in normal splenic B lymphocytes: 1.7% (3/180 cells). Similar findings were obtained for PCT4 (not shown).

All of the PCTs included in Table 1 arose in mice that were hemizygous for the $iGFP^{5'Myc}$ transgene, thus carrying one targeted *Myc* locus and one normal *Myc* locus. To show directly that the GFP^+ tumors used the targeted *Myc* allele for genetic recombination with *Igh*, we refined our PCR analysis of der(15) by replacing the *Myc* primer used for detecting the underlying *Igh–Myc* junction with a GFP primer that annealed further upstream (~2 kb) of *Myc* (Figure 1, green arrow below the scheme of der[15]). We combined the GFP primer with a PCR primer that annealed to the J_H portion of *Igh* (black arrow) and were readily able, in all four tumors (PCTs 1–4), to elongate the clonotypic *Igh–Myc* junction previously generated using the J_H and *Myc* exon 1 primer pair (red arrow). The der(12)-specific GFP–Myc–J_H fragments are shown in Figure 3d, lanes 1–4.

These results showed that in four independent tumors (PCTs 1–4), GFP activation was caused by juxtaposition of the V_H-GFP gene to *Igh* enhancers following chromosomal T(12;15) translocation.

We predicted that, in contrast to the four GFP^+ tumors described above, the GFP^- neoplasms had used the normal rather than the targeted *Myc* allele for translocation with *Igh*. Consistent with this possibility, we failed to detect GFP–Myc–J_H junctions in PCTs 6–8 (Figure 3d). In the case of PCTs 10 and 11, however, clonotytpic GFP–Myc–J_H junctions were obtained (Figure 3d). This suggested that the targeted *Myc* allele had recombined with *Igh*, yet GFP had not been activated. Lack of GFP expression could potentially be due to (1) epigenetic changes that diminish or extinguish GFP expression by silencing the *Igh–Myc* chromatin domain or (2) genetic changes such as translocation breakpoints disrupting the Eμ enhancer or—in keeping with the role of activation-induced cytidine deaminase in the origin of the T(12;15) translocation (Ramiro *et al.*, 2004; Franco *et al.*, 2006)—crippling activation-induced cytidine deaminase-mediated point mutations in the V_H promoter or the coding sequence of the GFP gene (Muramatsu *et al.*, 2000).

As molecular analyses, including DNA sequencing of translocation breakpoint regions, have not supported any of these possibilities thus far, alternative explanations must be considered

to account for the apparent absence of GFP expression in PCTs 10 and 11. The most likely of those postulates the co-existence of a frank GFP^- neoplasm and incipient GFP^+ tumor cell clones in the same mouse. According to this explanation, the mice contained an overt $CD138^+$ plasma cell tumor, designated PCT 10 or 11, that was readily detected by flow cytometry, yet lacked GFP expression either because it contained an unusual T(12;15) exchange that was not detectable with the PCR methods used here, harbored a variant *Myc* translocation that used an immunoglobulin light-chain instead of the *Igh* locus, or did not harbor an *Myc* translocation at all. Be this as it may, both mice additionally contained at least one $T(12;15)^+$ cell clone that had used the GFP-targeted *Myc* allele for recombination with *Igh* (based on the PCR results shown in Figure 3d) and, hence, expressed GFP. However, due to the small size of the underlying cell clone, the GFP^+ cells remained undetected by FACS. Consistent with this theory, clonal diversity of $T(12;15)^+$ PCTs has been repeatedly documented in strain C mice undergoing peritoneal tumor induction (Janz *et al.*, 1993; Müller *et al.*, 1996, 1997a; Kovalchuk *et al.*, 2000a, b, 2003). Furthermore, it is well established that PCR analysis of clonotypic *Myc*-*Igh* junctions detects T(12;15) translocation-bearing cells with much greater sensitivity than possible with FACS analysis of GFP expression in $iGFP^{5'Myc}$ mice. PCR routinely detects one $T(12;15)^+$ cell among 10^5–10^6 normal cells (Janz, 2006), whereas conventional flow cytometry detects one GFP^+ cell among 10^2–10^3 normal cells. The large difference in the detection limit (two to three orders of magnitude) of scoring $T(12;15)^+$ cells by PCR versus FACS analysis would thus explain the findings in PCT10/11-carrying mice without postulating that the GFP reporter had failed.

As stated above, a follow-up study producing a larger sample of $T(12;15)^+$ tumors in $iGFP^{5'Myc}$ mice is necessary before it can be determined with which frequency, if any, the GFP-targeted *Myc* locus undergoes T(12;15) exchange without activating the GFP reporter. Using to that end homozygous transgenic $iGFP^{5'Myc}$ mice may be particularly productive, because in these mice only GFP-targeted *Myc* alleles are available for T(12;15) exchange.

The newly developed $iGFP^{5'Myc}$ mice provide proof of principle that the targeted insertion of a transgenic reporter in the vicinity of an oncogene is a viable approach for detecting, enumerating and studying translocation-bearing cells in their normal tissue context. Combined with sensitive *in vivo* imaging techniques, such as two-photon microscopy (Germain *et al.*, 2005; Wessels *et al.*, 2007), the $iGFP^{5'Myc}$ mice may afford the possibility to visualize the migration and trafficking of *Igh–Myc* translocation-carrying cells *in vivo*. Additional questions that can be readily addressed with the assistance of the GFP reporter include the abundance and tissue distribution of $T(12;15)^+$ tumor cells, using fluorescence microscopy, immunohistochemistry, flow cytometry and whole-body fluorescence imaging. Still more interesting are questions that might be attacked in future studies on translocation-carrying B-lineage cells that have not yet completed malignant transformation. Figure 4, which depicts our most recent findings in tumor-free $iGFP^{5'Myc}$ mice, suggests that the GFP reporter may have great potential in that regard. Thus, 8 to 9-month-old tumor-free $iGFP^{5'Myc}$ mice hyper-immunized with the T-cell-dependent antigen, sheep red blood cells, showed a nearly threefold increase in the number of GFP-expressing $B220^+CD19^+$ splenocytes (0.12%) compared with age-matched non-immunized $iGFP^{5'Myc}$ mice (0.041%) and normal C mice (0.0088%) used as background controls. The result implicates the germinal center reaction in the promotion of GFP^+ cells and, hence, $T(12;15)^+$ B-lymphocytes that can be operationally defined as pre-malignant PCT precursors.

Relatively simple questions to be asked initially in follow-up studies include whether ‘pre-malignant’ $T(12;15)^+$ cells are scattered in lymphoid tissues or clustered in certain anatomical sites, such as germinal centers. A similarly trivial question is whether $T(12;15)^+$ cells can also reside in non-lymphoid tissues; for example, the lamina propria of the gut, as suggested by PCR results obtained in our laboratory (Müller *et al.*, 1997a, b). Somewhat

more involved will be attempts to pinpoint the stage(s) of B-cell differentiation at which translocations take place: T(12;15) caused by V(D)J recombination may occur in immature B cells in the bone marrow, whereas translocations caused by aborted isotype switching and VDJ hypermutation may take place in mature B cells in secondary lymphoid tissues (Wang *et al.*, 2009). A third set of studies will focus on the mechanism of translocation (Gostissa *et al.*, 2009a); for example, crossing the iGFP$^{5'Myc}$ reporter on genetic backgrounds that contain certain activation-induced cytidine deaminase (Cheng *et al.*, 2009) or DNA double-strand break repair mutations (Nussenzweig *et al.*, 1997; Ouyang *et al.*, 1997; Difilippantonio *et al.*, 2000) may provide important insights into the role of these pathways in the origin of T(12;15). Similarly, breeding the iGFP reporter onto certain cytokine including IL-6 transgenic (Suematsu *et al.*, 1992) backgrounds may enhance our understanding of growth, differentiation and survival requirements of aberrant T(12;15)$^{+}$ cell clones.

In conclusion, extension of the present reporter gene insertion approach to the pre-malignant state (*Igh–Myc*-bearing tumor precursors) and to other types of oncogene-activating or fusion-gene translocations (Mitelman *et al.*, 2007) may lead to fundamental new insights into the nature, developmental stage and site of origin of tumor progenitors that are of great relevance for human cancer.

Supplementary Material

Refer to Web version on PubMed Central for supplementary material.

Acknowledgments

We thank our colleagues from NCI and NIAID, NIH for their contributions to this project: Tina Willington, Vaishali Jarral and Wendy DuBois for genotyping and assistance with the mouse experiments; Eileen Southon for gene targeting; Dr Alexander L Kovalchuk for advice on PCR analysis and providing primers; Drs Sung Sup Park and Santiago Silva for contributions to early stages of this project; and Drs Michael Potter and Beverly Mock for stimulating discussion and laboratory support. For assistance with transfer, cryopreservation, maintenance and rederivation of mice under SPF conditions, we thank: Ling Hu, CCOM, Iowa City, Iowa; the staff of the Jackson Laboratory, Bar Harbor, Maine; and the Office of Animal Resources, CCOM, particularly Dr Kem Singletary and James Hynes. We also thank Lorraine Tygrett, CCOM for assistance with flow cytometry. This work was supported, in part, by the Intramural Research Program of the NIH (LT, RC, TR) and Award Number P50CA097274 from the National Cancer Institute (SJ).

References

Anderson PN, Potter M. Induction of plasma cell tumours in BALB-c mice with 2,6,10,14-tetramethylpentadecane (pristane). Nature. 1969; 222:994–995. [PubMed: 5789334]

Cheng HL, Vuong BQ, Basu U, Franklin A, Schwer B, Astarita J, et al. Integrity of the AID serine-38 phosphorylation site is critical for class switch recombination and somatic hypermutation in mice. Proc Natl Acad Sci USA. 2009; 106:2717–2722. [PubMed: 19196992]

Dalla-Favera R, Bregni M, Erikson J, Patterson D, Gallo RC, Croce CM. Human c-myc onc gene is located on the region of chromosome 8 that is translocated in Burkitt lymphoma cells. Proc Natl Acad Sci USA. 1982; 79:7824–7827. [PubMed: 6961453]

Difilippantonio MJ, Zhu J, Chen HT, Meffre E, Nussenzweig MC, Max EE, et al. DNA repair protein Ku80 suppresses chromosomal aberrations and malignant transformation. Nature. 2000; 404:510–514. [PubMed: 10761921]

Eisenman RN. Deconstructing myc. Genes Dev. 2001; 15:2023–2030. [PubMed: 11511533]

Franco S, Gostissa M, Zha S, Lombard DB, Murphy MM, Zarrin AA, et al. H2AX prevents DNA breaks from progressing to chromosome breaks and translocations. Mol Cell. 2006; 21:201–214. [PubMed: 16427010]

Germain RN, Castellino F, Chieppa M, Egen JG, Huang AY, Koo LY, et al. An extended vision for dynamic high-resolution intravital immune imaging. Semin Immunol. 2005; 17:431–441. [PubMed: 16216522]

Gostissa M, Ranganath S, Bianco JM, Alt FW. Chromosomal location targets different MYC family gene members for oncogenic translocations. Proc Natl Acad Sci USA. 2009a; 106:2265–2270. [PubMed: 19174520]

Gostissa M, Yan CT, Bianco JM, Cogne M, Pinaud E, Alt FW. Long-range oncogenic activation of Igh-c-myc translocations by the Igh 3′ regulatory region. Nature. 2009b; 462:803–807. [PubMed: 20010689]

Janz S. Myc translocations in B cell and plasma cell neoplasms. DNA Repair (Amst). 2006; 5:1213–1224. [PubMed: 16815105]

Janz S, Müller J, Shaughnessy J, Potter M. Detection of recombinations between c-myc and immunoglobulin switch alpha in murine plasma cell tumors and preneoplastic lesions by polymerase chain reaction. Proc Natl Acad Sci USA. 1993; 90:7361–7365. [PubMed: 8346257]

Kovalchuk AL, Kim JS, Janz S. E mu/S mu transposition into Myc is sometimes a precursor for T(12;15) translocation in mouse B cells. Oncogene. 2003; 22:2842–2850. [PubMed: 12743607]

Kovalchuk AL, Kishimoto T, Janz S. Lymph nodes and Peyer's patches of IL-6 transgenic BALB/c mice harbor T(12;15) translocated plasma cells that contain illegitimate exchanges between the immunoglobulin heavy-chain mu locus and c-myc. Leukemia. 2000a; 14:1127–1135. [PubMed: 10865979]

Kovalchuk AL, Müller JR, Janz S. Deletional remodeling of c-myc-deregulating translocations. Oncogene. 1997; 15:2369–2377. [PubMed: 9393881]

Kovalchuk AL, Mushinski EB, Janz S. Clonal diversification of primary BALB/c plasmacytomas harboring T(12;15) chromosomal translocations. Leukemia. 2000b; 14:909–921. [PubMed: 10803525]

Kuppers R, Dalla-Favera R. Mechanisms of chromosomal translocations in B cell lymphomas. Oncogene. 2001; 20:5580–5594. [PubMed: 11607811]

Levens DL. Reconstructing MYC. Genes Dev. 2003; 17:1071–1077. [PubMed: 12730130]

Mitelman F, Johansson B, Mertens F. The impact of translocations and gene fusions on cancer causation. Nat Rev Cancer. 2007; 7:233–245. [PubMed: 17361217]

Müller JR, Jones GM, Janz S, Potter M. Migration of cells with immunoglobulin/c-myc recombinations in lymphoid tissues of mice. Blood. 1997a; 89:291–296.

Müller JR, Jones GM, Potter M, Janz S. Detection of immunoglobulin/c-myc recombinations in mice that are resistant to plasmacytoma induction. Cancer Res. 1996; 56:419–423. [PubMed: 8542601]

Müller JR, Mushinski EB, Jones GM, Williams JA, Janz S, Hausner PF, et al. Generation of immunoglobulin/c-myc recombinations in murine Peyer's patch follicles. Curr Top Microbiol Immunol. 1997b; 224:251–255.

Muramatsu M, Kinoshita K, Fagarasan S, Yamada S, Shinkai Y, Honjo T. Class switch recombination and hypermutation require activation-induced cytidine deaminase (AID), a potential RNA editing enzyme. Cell. 2000; 102:553–563. [PubMed: 11007474]

Nussenzweig A, Sokol K, Burgman P, Li L, Li GC. Hypersensitivity of Ku80-deficient cell lines and mice to DNA damage: the effects of ionizing radiation on growth, survival, and development. Proc Natl Acad Sci USA. 1997; 94:13588–13593. [PubMed: 9391070]

Ouyang H, Nussenzweig A, Kurimasa A, Soares VC, Li X, Cordon-Cardo C, et al. Ku70 is required for DNA repair but not for T cell antigen receptor gene recombination in vivo. J Exp Med. 1997; 186:921–929. [PubMed: 9294146]

Ramiro AR, Jankovic M, Eisenreich T, Difilippantonio S, Chen-Kiang S, Muramatsu M, et al. AID is required for c-myc/IgH chromosome translocations in vivo. Cell. 2004; 118:431–438. [PubMed: 15315756]

Robbiani DF, Bothmer A, Callen E, Reina-San-Martin B, Dorsett Y, Difilippantonio S, et al. AID is required for the chromosomal breaks in c-myc that lead to c-myc/IgH translocations. Cell. 2008; 135:1028–1038. [PubMed: 19070574]

Silva S, Kovalchuk AL, Kim JS, Klein G, Janz S. BCL2 accelerates inflammation-induced BALB/c plasmacytomas and promotes novel tumors with coexisting T(12;15) and T(6;15) translocations. Cancer Res. 2003; 63:8656–8663. [PubMed: 14695177]

Suematsu S, Matsusaka T, Matsuda T, Ohno S, Miyazaki J, Yamamura K, et al. Generation of plasmacytomas with the chromosomal translocation t(12;15) in interleukin 6 transgenic mice. Proc Natl Acad Sci USA. 1992; 89:232–235. [PubMed: 1729694]

Wang JH, Gostissa M, Yan CT, Goff P, Hickernell T, Hansen E, et al. Mechanisms promoting translocations in editing and switching peripheral B cells. Nature. 2009; 460:231–236. [PubMed: 19587764]

Wessels JT, Busse AC, Mahrt J, Dullin C, Grabbe E, Mueller GA. In vivo imaging in experimental preclinical tumor research—a review. Cytometry A. 2007; 71:542–549. [PubMed: 17598185]

Willis TG, Dyer MJ. The role of immunoglobulin translocations in the pathogenesis of B-cell malignancies. Blood. 2000; 96:808–822. [PubMed: 10910891]

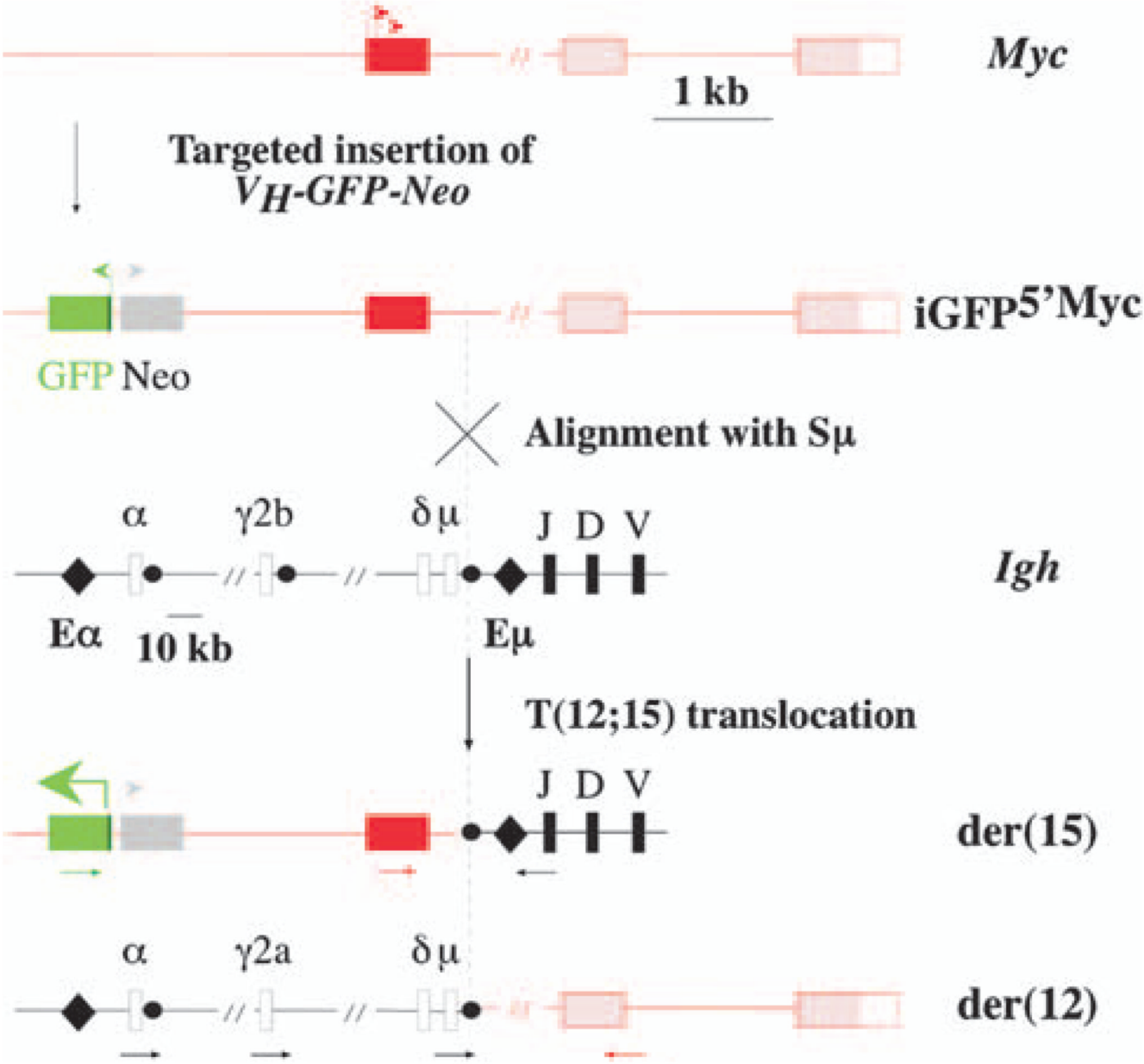

Figure 1.

Genetic system for detection of the T(12;15) translocation in B-lineage cells of iGFP5′Myc gene-insertion mice. Shown above are schematic representations of the normal mouse *Myc* locus on chromosome 15, and of the targeted *Myc* locus carrying the inserted V_H-GFP-Neo gene in iGFP$^{5'Myc}$ knock-in mice. The non-coding first exon of *Myc* is depicted by a red box, with the P1 and P2 *Myc* promoters indicated by two red arrows pointing right. The coding region of *Myc* (exons 2 and 3) and the 3′ untranslated region of *Myc* exon 3 are depicted by two pink boxes and one white box, respectively. The 1.6-kb first intron of *Myc* is not drawn to scale (as indicated by the short, oblique double line). The transcriptional orientations of the inserted GFP and Neo genes are indicated by colored arrows at transcriptional start sites. Shown in center is a schematic representation of the *Igh* locus on chromosome 12. The *Igh* variable (V_H), diversity (D) and joining (J_H) regions are

represented by thick vertical lines labeled as such. The *Igh* constant region (C_H), which is flanked by the intronic heavy-chain enhancer (Eμ) and the 3′ Cα heavy-chain enhancer (Eα; indicated by two black diamonds), is only partially represented by four C_H genes: Cμ, Cα, Cγ2b and Cα (white, labeled boxes). The corresponding switch regions are indicated by black dots (except in the case of Cδ, which does not have a canonical switch region). Four additional genes in the mouse C_H cluster (Cγ1, Cγ2a, Cγ3, Cε) are not shown. The *Igh* locus and the targeted *Myc* locus are aligned at a crossover site typically used to generate the T(12;15) translocation: the switch μ region on chromosome 12 and the first intron of *Myc* on chromosome 15. This is denoted by a cross-labeled alignment with Sμ. The actual site of DNA double-strand breakage and reciprocal transchromosomal recombination is indicated by a vertical, dashed line and an arrow-labeled T(12;15) translocation. Shown at bottom are schematic representations of the reciprocal products of the translocation: der(15) and der(12). Juxtaposition of Eμ to the V_H promoter of the GFP gene leads to the expression of GFP on der(15), as indicated by a thick green arrow pointing left. Annealing sites for PCR primers in *Igh*, *Myc* and V_H-GFP used to detect reciprocal *Igh–Myc* junctions on der(12) and *Igh–Myc–GFP* junctions on der(15) are indicated by horizontal arrows that are colored black, red and green, respectively.

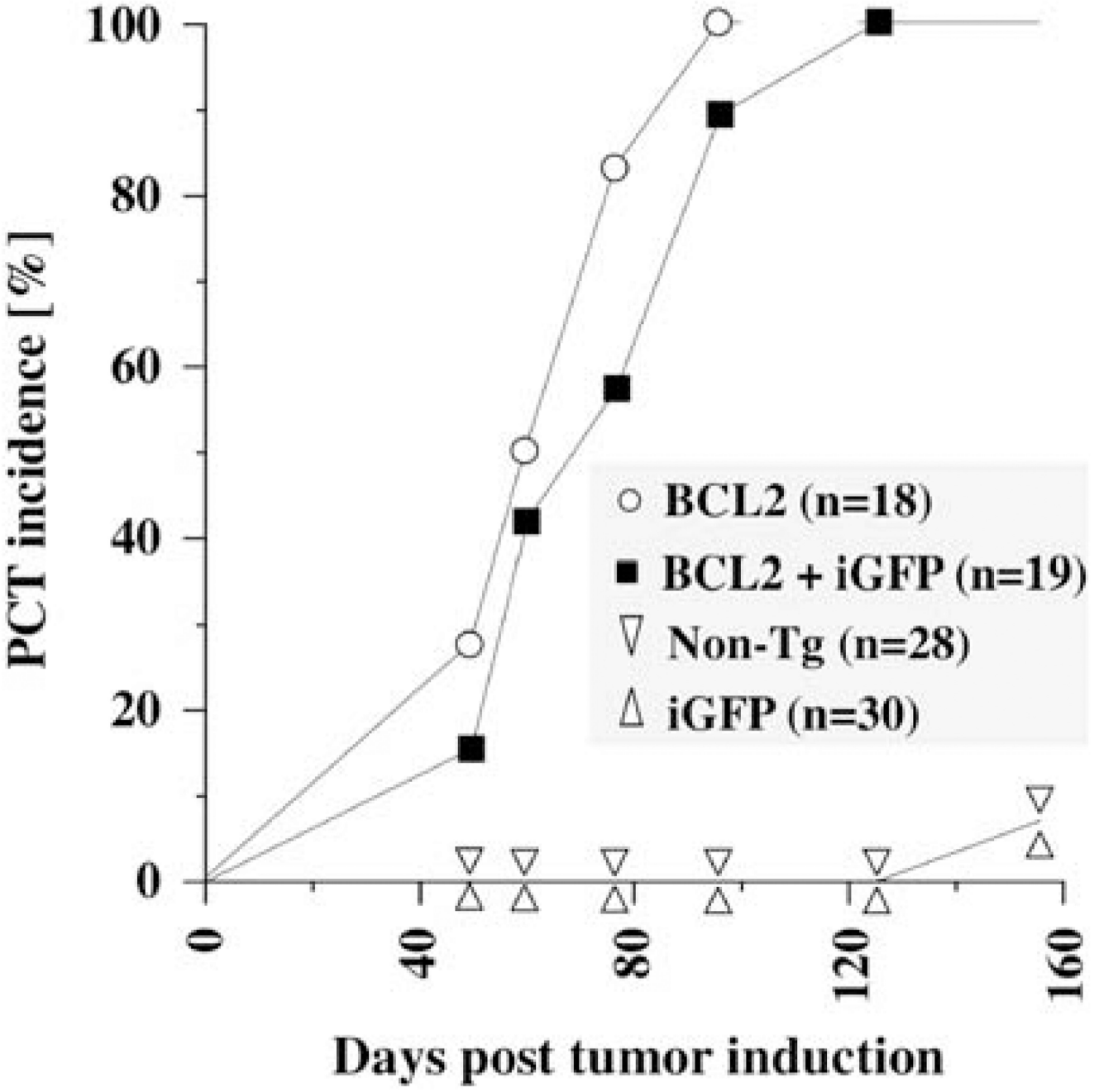

Figure 2.

The iGFP$^{5'Myc}$ translocation reporter does not affect the genetic susceptibility of mice to plasmacytoma development. Depicted are onset and incidence of inflammation (pristane)-induced peritoneal plasmacytoma (PCT) in double-transgenic C.iGFP$^{5'Myc}$/BCL2 mice (squares) and single-transgenic C.BCL2 mice (circles). In both strains, the BCL2 transgene accelerated PCT development with the same efficiency as observed in a previous study (Silva *et al.*, 2003). Single transgenic C.iGFP$^{5'Myc}$ mice (triangles pointing up) and non-transgenic littermates (triangles pointing down), in which tumor development began just before termination of the study, on day 160 after tumor induction with pristane were

included as controls. In all mice, PCTs were detected by finding neoplastic plasma cells in ascites-cell specimens that had been stained according to Wright–Giemsa.

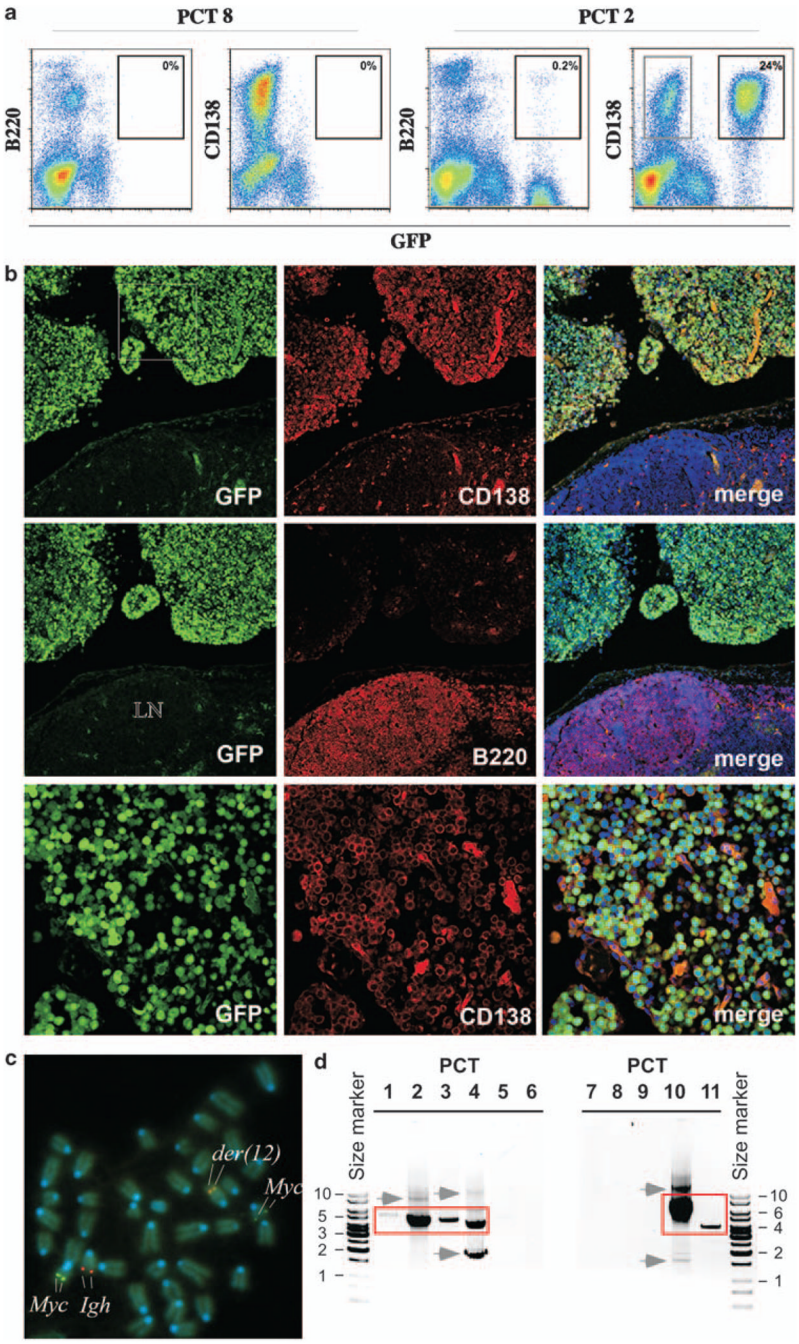

Figure 3.

Plasma-cell tumors in iGFP$^{5'Myc}$ mice express GFP consequent to T(12;15) translocation. (**a**) GFP expression in tumor cells, as detected by flow cytometry. Shown are scatter plots of ascites cells from mice bearing PCT8 (left, negative control) and PCT2 (right). Cells were treated with an Fc blocker (antibody to CD16/CD32) and stained with an antibody to B220 (CD45R; RA3–6B2) or CD138 (281–2). Isotype-matched antibodies of unrelated specificity confirmed the specificity of the B220 and CD138 signals. Cells were analyzed on a Beckman Coulter FC 500 instrument (Beckman Coulter Inc., Fullerton, CA, USA) using FlowJo software. Note the substantially expanded CD138^{+}GFP^{-} population of tumor cells (indicated by grey rectangle; 9% of all cells) that co-existed with the predominant

$CD138^{+}GFP^{+}$ tumor cell clone (24%) in the PCT2-harboring mouse. (**b**) GFP expression in $T(12;15)^{+}CD138^{+}$ tumor cells, as detected by immunofluorescence microscopy. Shown in the top and center rows are confocal microscopy images of serial tissue sections of a peritoneal granuloma that was labeled with PE-conjugated antibody to CD138 or B220, followed by counterstaining with DAPI (blue). These images are shown at low magnification. Adjacent to the granuloma (upper half of each image) is a piece of the mesenteric lymph node (MLN, lower half of each image). The three images in the top row show that plasma cells expressing GFP (left panel) and CD138 (center panel) had infiltrated the granuloma in large numbers, but were rare (scattered) in the MLN. The images in the center row reveal $B220^{+}GFP^{-}$ B cells that populate the MLN but not the granuloma. The bottom-row images present the $CD138^{+}GFP^{-}$ tumor cells included in the white square in the upper left-hand panel taken at higher magnification. (**c**) Presence of the T(12;15), as detected by FISH. Metaphase chromosome spread of PCT 1 hybridized to FISH probes for *Myc* (FITC, green, Chr 15) and *Igh* (Cy5, red, Chr 12). der(12) is indicated by co-localization of FISH signals, whereas der(15) is visualized by the weak *Myc* signal to the upper right of the image. Chromosomes were counter-stained with DAPI (blue). (**d**) Rearrangement of GFP-targeted *Myc* allele with *Igh* as detected by PCR analysis. Shown are der(15)-typical GFP–Myc–Igh junction fragments (red rectangles) detected in PCT1–4 and PCT10–11 by PCR analysis of genomic DNA. Junction fragments were size fractionated in an agarose gel and confirmed to be clonotypic by DNA sequence analysis of the underlying DNA recombination (not shown). PCR fragments outside of the red boxes, the most prominent of which are indicated by grey arrows pointing right, are either artifacts or *bona fide* translocation junction fragments indicating the clonal diversity of incipient PCTs in strain C mice. Size markers (kb) are indicated.

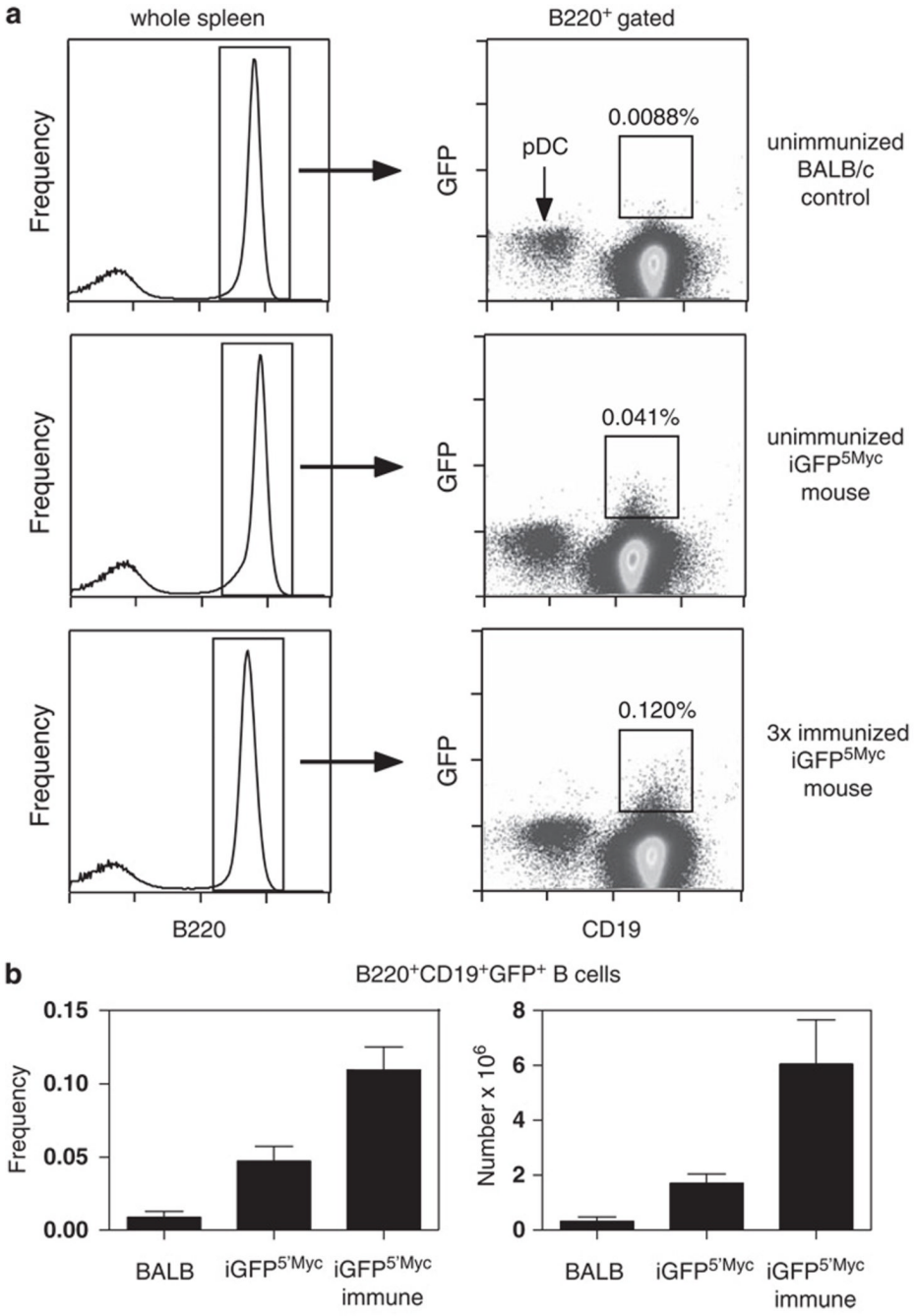

Figure 4.

Flow cytometric detection of GFP^+ splenic B cells from C.$iGFP^{5'Myc}$ mice. Viable mononuclear spleen cell suspensions from unimmunized BALB/c (C) control, unimmunized C.$iGFP^{5'Myc}$, or SRBC hyperimmunized C.$iGFP^{5'Myc}$ mice were prepared and stained with anti-B220 and anti-CD19 mAbs, as described in Supplementary Methods. Cells were analyzed on a BD FACSCanto with 3×10^6 events collected per sample to ensure detection of rare events. Using FlowJo analysis software, viable single cells were carefully selected using forward versus side scatter, followed by forward scatter versus forward scatter pulse width gating. (**a**) Representative plots from unimmunized C, unimmunized C.$iGFP^{5'Myc}$ and hyperimmunized C.$iGFP^{5'Myc}$ mice are shown. Representative CD19 versus GFP bivariate

plots (right panels) derived from the $B220^+$ gate (left panels) are illustrated. The square gates used to calculate the frequency of $B220^+CD19^+GFP^+$ events are shown on the CD19 versus GFP plots. Note that $CD19^-$ plasmacytoid dendritic cells (pDC) are present within the $B220^+$ gate. Their identity was confirmed with CD11c staining (data not shown). (**b**) Graphs represent the frequency of $CD19^+GFP^+$ B cells within the $B220^+$ gated population (left panel) and the total number of $B220^+CD19^+GFP^+$ cells per spleen (right panel). BALB, unimmunized C control; $iGFP^{5'Myc}$, unimmunized $C.iGFP^{5'Myc}$; $iGFP^{5'Myc}$ immune, hyperimmunized $C.iGFP^{5'Myc}$. Values obtained from C control mice represent background levels. Bar graphs = mean ± s.d.; n = 3–4 per group.

Table 1

Analysis of PCT

PCT[a]	GFP[b]	der(12)[c]	der(15)[d]	GFP-Myc[e]
1	+	+	+	+
2	+	+	+	+
3	+	ND	+	+
4	+	+	+	+
5	−	+	ND	ND
6	−	+	+	−
7	−	+	+	−
8	−	+	+	−
9	−	+	ND	ND
10	−	+	+	+
11	−	+	+	+

Abbreviations: PCT, plasmacytomas; GFP, green fluorescent protein; *Igh–Myc*, *Myc*-deregulating chromosomal T(12;15); ND, not detected.

[a] Periotoneal PCTs produced by injecting double-transgenic C.iGFP$^{5'Myc}$/BCL2 mice intraperitoneally with 0.2 ml pristane (2,6,10,14-tetramethylpentadecane). Tumor incidence and onset are depicted in Figure 2.

[b] GFP expression in tumor cells as assessed by FACS analysis of ascites cell specimens and immunofluorescence microscopy of peritoneal granulomas, as illustrated in Figure 3 and Supplementary Figure 2.

[c] *Igh–Myc* junctions indicative of the *Myc*-deregulating product of the T(12;15) translocation, der(12), as detected by PCR analysis using the *Myc* exon 2 and *Igh* C_H PCR primers indicated in Figure 1, bottom.

[d] *Igh–Myc* junctions indicative of the reciprocal product of the T(12;15) translocation, der(15), as detected by PCR analysis using the *Myc* exon 1 (red) and J_H (black) PCR primers indicated in Figure 1, bottom.

[e] *Igh–Myc* junctions indicative of the reciprocal product of the T(12;15) translocation, der(15), as detected by PCR analysis using the GFP (green) and J_H (black) primers indicated in Figure 1, bottom.